Published in final edited form as:
Sci Transl Med. 2011 April 13; 3(78): 78ra31. doi:10.1126/scitranslmed.3001374.

IL-25 Causes Apoptosis of IL-25R–Expressing Breast Cancer Cells Without Toxicity to Nonmalignant Cells

Saori Furuta[1,2], **Yung-Ming Jeng**[1,3], **Longen Zhou**[1], **Lan Huang**[4,5], **Irene Kuhn**[2], **Mina J. Bissell**[2,*], and **Wen-Hwa Lee**[1,*]

[1]Department of Biological Chemistry, College of Medicine, University of California, Irvine, CA 92697, USA.

[2]Department of Cancer and DNA Damage Responses, Life Sciences Division, Lawrence Berkeley National Laboratory, Berkeley, CA 94720, USA.

[3]Department of Pathology, National Taiwan University Hospital, Taipei 100, Taiwan.

[4]Department of Physiology and Biophysics, College of Medicine, University of California, Irvine, CA 92697, USA.

[5]Departments of Developmental and Cell Biology, College of Medicine, University of California, Irvine, CA 92697, USA.

Abstract

As cells differentiate into tissues, the microenvironment that surrounds these cells must cooperate so that properly organized, growth-controlled tissues are developed and maintained. We asked whether substances produced from this collaboration might thwart malignant cells if they arise in the vicinity of normal tissues. Here, we identified six factors secreted by nonmalignant mammary epithelial cells (MECs) differentiating in three-dimensional laminin-rich gels that exert cytotoxic activity on breast cancer cells. Among these, interleukin-25 (IL-25/IL-17E) had the highest anticancer activity without affecting nonmalignant MECs. Apoptotic activity of IL-25 was mediated by differential expression of its receptor, IL-25R, which was expressed in high amounts in tumors from patients with poor prognoses but was low in nonmalignant breast tissue. In response to IL-25, the IL-25R on the surface of breast cancer cells activated caspase-mediated apoptosis. Thus, the IL-25/IL-25R signaling pathway may serve as a new therapeutic target for advanced breast cancer.

*To whom correspondence should be addressed. mjbissell@lbl.gov (M.J.B.); whlee@uci.edu (W.-H.L.).

Author contributions: W.-H.L. and M.J.B. were responsible for supervising the project and helping design the experiments. I.K. contributed to designing some of the control experiments. S.F. was responsible for designing and executing most of the experiments. Y.-M.J. analyzed the first cohort of breast cancer tissue sections and patients' clinical data. L.Z. performed mouse xenograft experiments. L.H. performed liquid chromatography–tandem mass spectrometry analysis. S.F., W.-H.L., M.J.B., and I.K. contributed to writing and revising the manuscript.

Competing interests: A patent (PCT/US2007/081395) has been filed related to the use of IL-25 for cancer treatment. All authors declare that they have no competing interests.

SUPPLEMENTARY MATERIAL

www.sciencetranslationalmedicine.org/cgi/content/full/3/78/78ra31/DC1 Materials and Methods
Table S1. Oligonucleotide sequences used in this study.
Fig. S1. Strong IL-25R staining in breast cancer cells as detected by a second IL-25R antibody.
Fig. S2. Indirect immunoaffinity purification of IL-25.
Fig. S3. Cell-killing activity of recombinant versus purified human IL-25 protein in breast cancer cells in conventional cultures.
Fig. S4. IL-17B is up-regulated in a subset of breast cancer cell lines and tissues and is important for their growth and invasive potentials.
References

INTRODUCTION

Normal epithelial cells play active and critical roles in the maintenance of tissue homeostasis. These cells regulate the secretion of autocrine and paracrine factors that promote the development of healthy organs and prevent aberrant growth of neighboring cells. We showed previously that in nonmalignant mammary epithelial cells (MECs), the breast cancer–associated gene 1 (BRCA1) protein forms a transcriptional repressor complex with the C-terminal binding protein interacting protein (CtIP) and the zinc finger protein ZBRK1 that suppresses *angiopoetin-1* gene expression, which in turn inhibits angiogenesis in neighboring endothelial cells (1). During mammary gland development, MECs produce substances that inhibit epithelial growth, including mammary-derived growth inhibitor and transforming growth factor–β (2). In the mammary gland, myoepithelial cells contribute to basement membrane formation and tissue polarity and secrete anti-invasive and antiangiogenic factors, including maspin and laminin-111 (3, 4). We asked whether normal MECs also secrete factors that directly and specifically inhibit malignant cell growth and/or survival and, if so, what are the underlying mechanisms for this intrinsic antitumor activity.

We showed previously that conditioned medium (CM) from nonmalignant MECs in the process of forming acini in three-dimensional (3D) laminin-rich extracellular matrix (lrECM) gels “reverts” the malignant phenotype of breast cancer cells to basally polarized, growth-suppressed (dormant), acinar-like structures; this phenotypical reversion was also shown with cell signaling inhibitors such as a β_1 integrin–blocking antibody (5, 6). These observations suggest that acinus-forming nonmalignant MECs secrete factors that can suppress the phenotype of breast cancer cells growing in 3D cultures. We hypothesized that such complex phenotypical reversion is likely a result of multiple signaling factors that in combination allow cancer cells to form quiescent acinar-like structures.

Here, we sought to identify and characterize these factors using size fractionation of the CM from nonmalignant cells and functional assays to identify the active molecules. However, fractionation revealed that the CM could be divided into morphogenic activity in the insoluble fraction and cytotoxic activity in the soluble fraction. Here, we characterized the molecule with the most potent tumor cell–killing activity in the 10- to 50-kD fraction, which proved to be interleukin-25 (IL-25). We then showed that this cytokine is active against breast cancer cells that express high amounts of the cognate receptor, IL-25R, and that treatment of these cells with IL-25 caused the receptor to interact with death domain (DD)–associating proteins, activating caspase-mediated apoptosis.

To determine the relevance of the above findings to breast cancer, we measured the levels of IL-25R in two separate tissue cohorts derived from breast cancer patients and found that high levels of IL-25R correlated with poor prognosis. These data suggest strongly that the IL-25/IL-25R signaling pathway may provide novel targets for treating aggressive breast cancers.

RESULTS

Factors secreted from differentiating MECs kill breast cancer cells

To identify and characterize the components secreted by the nonmalignant cells, we fractionated their CM by solubility and molecular size. Each fraction of the CM was replenished with essential growth factors (7) and used instead of the usual media to culture MCF7 breast cancer cells in 3D lrECM (Fig. 1A). The reverting/dormancy-inducing activity of the total CM could be separated into two complementary activities: morphogenic activity in the pellet fraction and cytotoxic activity in the soluble fraction. The pellet fraction caused

breast cancer cells to form spheroid structures reminiscent of differentiating MECs, although larger in size; this phenotype was distinct from those observed in breast cancer cells treated with total CM.

In contrast, the soluble fraction was cytotoxic for breast cancer cells (Fig. 1A), and this activity was further enriched in the 10- to 50-kD fraction. When treated with this fraction alone, there were no viable cells after 1 week (Fig. 1C). None of the CM fractions applied to the nonmalignant MCF10A cells in 3D cultures resulted in cell-killing activity (Fig. 1, B and C). These observations indicate that, whereas differentiating MECs secrete factors in the 10- to 50-kD range that exhibit tumor cell–specific cytotoxic activity, the nonmalignant cells themselves are resistant to such activity. The highest tumor cell–killing activity was detected in CM from MECs that had been differentiating for 4 days in the 3D cultures; this time scale corresponds to the midpoint in the process of acini formation (Fig. 1D). The result suggests that secretion of the cytotoxic factors for cancer cells is intimately linked to the progression of differentiation in 3D cultures and that the activity is effective on all the cancer cell lines tested.

Identification of factors secreted into the 10- to 50-kD CM

To identify proteins specifically secreted by differentiating MECs, but not by breast cancer cells, we analyzed the 10- to 50-kD CM fraction (day 4) from differentiating MCF10A cells and that from MCF7 breast cancer cells also cultured in 3D lrECM by mass spectrometry using 2D liquid chromatography (8). Through comparative analyses, we identified six differentially expressed factors, including antiangiogenic proteins [antithrombin III (ATIII) and vitamin D–binding protein (VBP) (9, 10)], proinflammatory cytokines [IL-1F7 and IL-25 (also called IL-17E) (11, 12)], and growth and differentiation proteins [bone morphogenetic protein 10 (BMP10) and fibroblast growth factor 11 (FGF11) (13, 14)] (Fig. 2A).

To verify the contribution of these factors to tumor cell–killing activity, we immunodepleted the 10- to 50-kD cytotoxic fraction from days 3 to 4 with antibodies to the six factors individually and to p84 control protein. The depletion efficacy was assessed by immunoblots performed on the immunoprecipitates (Fig. 2B). The immunodepleted fraction was used to culture MCF7 breast cancer cells in 3D lrECM, and fresh fractions were applied every 24 hours for 1 week. Depletion of individual factors attenuated the cell-killing activity to a different degree (Fig. 2C). However, protection from cell-killing activity was especially pronounced for depletion of ATIII, IL-1F7, IL-25, and VBP, suggesting critical roles for each of these four factors in this process.

To determine which of the four factors contained the most potent activity, we used 293T cells to generate cell lines that stably expressed ATIII, IL-1F7, IL-25, and VBP at comparable levels, determined by analyses of RNAs (Fig. 2D) and protein levels in the media (15). Cells were seeded at the same density, and the collected CM was normalized to total protein concentrations and tested on MCF7 cells cultured in 3D lrECM. CM from cells that overexpressed ATIII, IL-1F7, and VBP showed a cytostatic effect. However, CM from cells that overexpressed IL-25 showed a strong cytotoxic activity on MCF7 (Fig. 2E) as well as on two additional breast cancer lines, T47D and MDA-MB468 (Fig. 2F). We therefore concentrated on the mechanism of the cytotoxic activity of IL-25 and its possible utility in treating malignant tumors. As expected, nonmalignant MCF10A cells were resistant to the cytotoxic activity of IL-25–containing CM (Fig. 2F). IL-25 expression in 3D cultures correlated with the cytotoxicity of the CM described above (Fig. 1D) and peaked at day 4 in culture as well (Fig. 2G).

To determine the physiological significance of these modulations, we analyzed IL-25 expression in vivo in mice and on sections of normal breast tissue. We compared human and mouse *IL-25* genes and found them to share similar regulatory elements in their promoter regions (Fig. 3A). Analysis of the mouse mammary glands as a function of the pregnancy cycle showed that IL-25 expression gradually increases after puberty at about 5 weeks up to mid-pregnancy (Fig. 3, B to E) but declines thereafter, suggesting that IL-25 is temporally regulated in developing mammary glands reminiscent of temporal regulation of IL-25 secretion during the differentiation process in 3D cultures (Fig. 2G). Once acini are formed either by mouse mammary glands at mid-pregnancy (Fig. 3, B to E) or by nonmalignant human breast cells in 3D cultures (Fig. 2G), IL-25 expression was diminished. Indeed, when we analyzed IL-25 expression in normal breast tissue sections ($n = 30$) by immunohistochemistry (IHC), IL-25 signal was almost undetectable (Fig. 3F).

Purified IL-25 kills cancer cells in culture and inhibits tumor growth in vivo

To ascertain whether the cytotoxic activity of IL-25–containing CM did indeed result from IL-25, we purified this cytokine from 293T cells that stably expressed IL-25. Because secreted IL-25 was expected to be highly glycosylated, as is the case for other interleukin family members (16), the total glycoproteins were affinity-purified and then separated by gel filtration (size exclusion) chromatography. Pooled protein fractions 21 to 23 contained similar amounts of IL-25 and bovine serum albumin (BSA) carrier protein. Otherwise, IL-25 was estimated to be 90 to 95% pure. Upon electrophoresis in a denaturing gel, glycosylated IL-25 migrated at a position that corresponded to ~48 kD (Fig. 4A).

To test the activity of this fraction, we treated four breast cancer cell lines (MCF7, MDA-MB468, SKBR3, and T47D) with different doses of IL-25. All four breast cancer cell lines were sensitive to the purified IL-25 fraction in colony-forming assays, with IC_{50} (median inhibitory concentration) values of ~10 ng/ml (500 pM; molecular size = 20 kD for the nonglycosylated protein) (Fig. 4B). In contrast, nonmalignant MCF10A cells were relatively resistant to IL-25 (Fig. 4B).

We tested the potency of IL-25 in vivo using xenografts of MDA-MB468 breast cancer cells grown in mammary fat pads of nude mice. The tumors were grown for 10 days and then were injected with vehicle (phosphate-buffered saline, $n = 7$) or IL-25 (300 ng, $n = 8$) once a day for 1 month. IL-25 significantly retarded growth of the tumors. After 1 month, the average size of IL-25–treated tumors was threefold smaller than that of control tumors ($P = 0.0016$) (Fig. 4C).

To assess the systemic stress/toxicity caused by the treatment, we measured the body weight of these mice and found no measurable difference between the control and the treated groups (Fig. 4D). In addition, at the end of the experiment, we performed gross pathological examinations of various organs from the untreated and IL-25–treated mice, including intestine, kidney, heart, lungs, liver, and stomach based on size, color, presence of cysts or any other gross lesions, as well as any signs of inflammatory reactions or invasion. No apparent pathologies were found in any of these mice. For more stringent safety tests, a fivefold higher dose of IL-25 (1.5 μg) was injected into the tail veins of C57 mice (vehicle: $n = 3$; IL-25: $n = 5$). Again, no signs of illness (lethargy or weight loss) were observed (15), indicating a lack of toxicity to nonmalignant tissues.

When tumors from IL-25–treated and untreated (control) MDA-MB468 xenografts were excised and histologically examined, the treated samples contained about 50% fewer actively dividing tumor cells (Fig. 4E, b and c) that exhibited an average mitotic index that was half that of untreated tumors (Fig. 4E, a) (0.63 ± 0.055 versus 1.1 ± 0.17, respectively, $P = 0.053$) (15). In some of the IL-25–treated mice, the tumors had regressed completely, and

the lesion contained only lymphocytic infiltrates (Fig. 4E, b and c). These findings suggest a potential utility of IL-25 as an antitumor agent.

Breast tumor cells express high amounts of IL-25R compared to nonmalignant cells

As a mechanistic explanation for the selective antitumor activity of IL-25 in mice, we speculated that IL-25–induced cytotoxicity might be attributed to the differential expression of IL-25R (also called IL-17RB) on breast cancer cells. To test this, we screened for IL-25R expression in a panel of breast cancer cell lines that displayed different characteristics. These included estrogen receptor (ER)–positive breast cancer cells, such as the MCF7, MDA-MB361, T47D, and ZR75 cell lines, and ER-negative breast cancer cells, such as the MCF10A, MDA-MB468,MB435-S, MB231, MB175-7, SKBR3, HS578T, HBL100, and HCC1937 cell lines (17). The analysis of transcripts by reverse transcription–polymerase chain reaction (RT-PCR) showed that IL-25R was expressed in higher amounts in all the breast cancer cell lines examined relative to nonmalignant breast cell line MCF10A. Nevertheless, the IL-25R mRNA levels were surprisingly different among the cancer cell lines (Fig. 5A). On the other hand, the IL-25R protein concentrations in the breast cancer cell lines were much more similar to each other than to IL-25R concentrations in MCF10A cells and in another nonmalignant cell line, telomerase-immortalized human mammary epithelial (tHME) cells (Fig. 5B). The low amounts of IL-25R measured in the nonmalignant MEC cell lines are consistent with the IL-25R distribution reported in a previous study for normal breast as well as other organs (11).

High amounts of IL-25R in breast cancer cells suggest that the receptor may confer a growth advantage to these cells. To examine this possibility, we depleted IL-25R from a panel of breast cancer cell lines using an IL-25R–specific small interfering RNA (siRNA) (Fig. 5C) and measured the ability of the resulting cells to grow anchorage independently in soft agar (Fig. 5, D and E). Reduction of IL-25R markedly inhibited (75 to 85%) the growth of all the cancer cell lines tested (Fig. 5E), indicating that IL-25R is important for their anchorage-independent growth. To ascertain that the impaired ability of soft agar growth did not involve an off-target effect, we assessed whether coexpression of an siRNA-resistant version of the *IL-25R* gene (*IL-25R RM*) could rescue the growth properties of cancer cells. We generated an *IL-25R RM* construct that expressed an mRNA transcript harboring four silent mutations. In addition, we designed two siRNAs, only one of which targeted the region containing the mutations (siRNA #1). Western analysis confirmed that the expression of IL-25R RM in MDA-MB468 cancer cells rescued the IL-25R protein concentrations after treatment with siRNA #1, but not with siRNA #2 (Fig. 5F). Paralleling the restored IL-25R protein concentrations, expression of IL-25R RM rescued the ability of MDA-MB468 cells to grow in soft agar after treatment with IL-25R siRNA #1, but not with siRNA #2 (Fig. 5G). These results provide clear evidence that IL-25R expression is directly responsible for anchorage-independent growth of breast cancer cells.

To determine the amount of IL-25R expression in human breast cancer specimens, we performed immunostaining using two different IL-25R antibodies on two cohorts of resected ductal invasive carcinoma samples. The slides for analysis were selected to include both tumor and nontumorous epithelia. Of the 69 samples in the first cohort, which consisted of paraffin-embedded breast cancer tissue sections analyzed with the first batch of antibody obtained from GeneTex (please refer to Materials and Methods), there was intense membranous staining of IL-25R in 18.8% of the tumor tissues analyzed (13 of 69) (Allred score: 6 to 8) (Fig. 5H, b1 to b3) (18); in contrast, all nontumorous regions examined (69 of 69) showed no or little staining (Allred score: 0 to 2) (Fig. 5H, a1 to a3). Positive IL-25R staining correlated significantly with poor prognosis and high mortality rate in this cohort ($P < 0.001$) (Fig. 5I). Unfortunately, additional supplies of the GeneTex IL-25R antibody were no longer available from the manufacturer, and of the other available IL-25R antibodies,

none could be used for IHC on paraffin sections (see Materials and Methods). On the basis of its accurate identification of IL-25R in a number of assays, we chose a second IL-25R antibody from R&D for our studies. We could use this antibody successfully for immunofluorescence (IF) and for IHC on frozen tissue sections. By IF, the R&D antibody, similar to the GeneTex antibody, revealed accentuated localization of IL-25R at the cell membrane of cultured breast cancer cells, albeit with some additional staining in the Golgi (fig. S1A). IHC staining on a cohort of frozen sections of breast tissue samples (10 nonmalignant and 20 malignant) revealed again tumor-specific staining (fig. S1B), as had the GeneTex antibody (Fig. 5H). Note that the staining of frozen sections did not reveal the same degree of membrane specificity or localization as the staining of paraffin sections (compare fig. S1B with Fig. 5H). Further specification of localization will need to await availability of additional paraffin-compatible antibodies. Nevertheless, these two sets of IHC staining reveal high levels of IL-25R in tumor tissues, but none in normal tissues. The data thus provide a strong rationale for the observed tumor specificity of IL-25R cytotoxicity and its role as a marker of malignant progression and poor patient prognosis.

IL-25 stimulates formation of a cell death–inducing complex that activates caspase-mediated apoptosis

IL-25/IL-25R signaling has been shown to induce a proinflammatory response in certain tissues such as lung fibroblasts (19). In breast cancer cells, on the other hand, we found that IL-25 induces cell death. We reasoned that if IL-25/IL-25R interaction can send a death signal in breast cancer cells, IL-25R may serve as the death receptor and contain a DD signature motif. We aligned the C-terminal region of IL-25R (amino acids 362 to 467) with DDs of the apoptosis-stimulating fragment (FAS) receptor (FAS-R: amino acids 205 to 293) and tumor necrosis factor (TNF) receptor 1 (TNF-R1: amino acids 352 to 441) and found that this region of IL-25R shares about 30% similarity with both DDs (Fig. 6A). The residues highly conserved among DD-containing proteins are similar to those in the C-terminal region of IL-25R, except for Trp72 (20) (see the numbering in Fig. 6A). Therefore, this region of IL-25R appears to have a DD-like motif. Other members of the IL-17 receptor family, IL-17RA and IL-17RC, lack such a DD-like motif (15).

To test whether IL-25 treatment induces receptor-mediated apoptosis of breast cancer cells, we treated MDA-MB468 and MCF10A cells, which express high and low amounts of IL-25R, respectively, with IL-25 (Fig. 5, A and B). In MDA-MB468 breast cancer cells, but not in nonmalignant MCF10A cells, IL-25 caused the cleavage of caspases 8 and 3 within 30 min and measurable cleavage of poly(ADP-ribose) polymerase (PARP) after 24 hours (Fig. 6B), indicating the activation of apoptosis. Two alternative preparations of IL-25 protein—either immunoaffinity-purified from mammalian cells (fig. S2) or commercially available bacterially produced recombinant protein—likewise exerted a potent proapoptotic effect on MDA-MB468 cells (fig. S3), corroborating the mode of action of this protein.

To further confirm that IL-25R indeed mediates the cell death signaling of IL-25, we depleted IL-25R fromMDA-MB468 cells with siRNAs, which completely inhibited the protein expression after 60 hours (Fig. 6C). In cells treated with control luciferase siRNAs, IL-25 treatment caused cleavage of caspase 3 and PARP, whereas in cells depleted of IL-25R, such phenomena were absent (Fig. 6D). These results substantiate the notion that the IL-25–dependent death signal is indeed mediated through activation of IL-25R.

We then explored how a death signal from IL-25 is transduced by the receptor. If IL-25R were to have a DD-like motif, it would interact with DD-associating proteins upon IL-25 binding. To test this hypothesis, we treated MDA-MB468 cells with IL-25 and analyzed for the interactions between IL-25R and DD adaptor proteins: FAS-associated protein with death domain (FADD) and TNF-R1–associated death domain protein (TRADD) (21). As a

positive control, we also tested the interaction of IL-25R with TNF receptor–associated factor 6 (TRAF6). TRAF6 was shown previously to be associated with IL-25R even in the absence of the ligand through its binding to the motif around Glu341 (Glu338 in mouse) of IL-25R (22), a region N-terminal to the putative DD-like motif (amino acids 362 to 467).

We found that total amounts of IL-25R, FADD, and TRADD were highly elevated upon IL-25 treatment (Fig. 6D; input level shown in Fig. 6E). Moreover, IL-25R strongly interacted with FADD and TRADD only after IL-25 addition, as detected by reciprocal immunoprecipitation with IL-25R and FADD antibodies (Fig. 6E). The increases in FADD, TRADD, and IL-25R protein concentrations in response to IL-25 treatment may indicate their activation and contribute to their apparent increased interactions. We confirmed that TRAF6 indeed remained associated with IL-25R even in the absence of the ligand. Despite the unchanged total amount of TRAF6, the amount of TRAF6 that coprecipitated with IL-25R increased in proportion to the elevated IL-25R concentrations upon IL-25 treatment (Fig. 6, D and E); these observations suggest that IL-25R and TRAF6 are always bound together, as previously observed in cells in which the two proteins were overexpressed ectopically (22). Moreover, reduction of FADD or TRADD in breast cancer cells with specific siRNAs largely impaired the proapoptotic activity of IL-25 (Fig. 6, F and G), suggesting that this function of IL-25 depends on the FADD and TRADD proteins. These results indicate that IL-25 binding to its receptor increases the stability of the IL-25R–associated complex, which contains FADD and TRADD. This complex then triggers the activation of caspase-mediated apoptosis.

IL-25–mediated apoptotic signaling depends on the DD-like region of IL-25R

To dissect how IL-25 sends death signals through IL-25R, we ectopically expressed inMCF10A cells either the wild-type IL-25R protein or a mutant from which either the TRAF6 binding domain (ΔTRAF6) or the DD-like region (ΔDD) was deleted (Fig. 7, A and B); MCF10A cells were otherwise resistant to apoptosis mediated by IL-25 (Fig. 6B). Upon IL-25 addition, MCF10A cells that overexpressed wild-type IL-25R displayed the apoptotic response characterized by cleavage of caspase 3 and PARP in a time-dependent manner (Fig. 7C), demonstrating that IL-25R expression is sufficient to render these cells sensitive to apoptotic effect of IL-25. In contrast, MCF10A cells that expressed the ΔDD IL-25R mutant remained resistant to the IL-25 death signal. This finding indicates that the DD-like region of IL-25R is essential for mediating the death signal of IL-25, a finding that is consistent with the increased association of IL-25R with DD adaptor proteins, FADD and TRADD, upon IL-25 treatment. Surprisingly, cells that expressed the ΔTRAF6 IL-25R mutant showed an elevated level of apoptosis even in the absence of IL-25 stimulation, suggesting that TRAF6 binding to IL-25R confers protection against apoptosis in MCF10A cells (Fig. 7C). These results reveal the presence of two functionally distinct apoptotic regulatory regions, a TRAF6-binding domain and a putative DD-like motif, in the C terminus of IL-25R, demonstrating the intricacy of the signaling cascades involved in ligand-activated IL-25R function.

DISCUSSION

It is long appreciated that the prevalence of cancer in human populations is far lower than one would predict based on DNA mutation rates (23). If oncogenic mutations are not sufficient to establish tumors, how are tumors contained, suppressed, or eliminated before they become evident? A number of tumor surveillance mechanisms have been described, including the classic molecular tumor suppressors, immune surveillance, and suppression by ECM and other microenvironmental factors. This study adds a new type of suppression to the list: factors secreted by normal differentiating cells that could kill or subdue their transformed counterparts.

We had shown previously that differentiating MECs secrete factors that allow phenotypic reversion of breast cancer cells, leading to formation of acinus-like structures and growth suppression (5). The secreted factors could be partitioned into soluble and insoluble fractions; the former had tumor cell–killing activity and the latter had most of the "reverting" activity. Here, we identified six factors in the soluble fraction that were secreted by differentiating MECs in 3D and shown to either kill or suppress the growth of tumor cells. This collection of factors included antiangiogenic proteins (ATIII and VBP), proinflammatory cytokines (IL-1F7 and IL-25), and growth and differentiation proteins (FGF11 and BMP10). IL-25 exhibited the most potent cytotoxic activity toward breast cancer cells, whereas the other factors exhibited cytostatic activity. Here, we focused on the mechanism of action of IL-25 and its potential as a therapeutic agent in breast cancer.

IL-25 is a proinflammatory cytokine that is expressed highly in certain organs, such as testis, prostate, and spleen, and is expressed in low amounts in other organs including normal breast (11, 24). It is the most distant member of the IL-17 family of proteins, sharing only 16 to 30% sequence homology with the other family members (25). It plays a role in proinflammatory responses of lymphatic, kidney, and lung cells by inducing production of T helper 2 (T_H2)–type cytokines (11, 19, 24, 26). The function of IL-25 in other tissues remains to be elucidated.

We show here that IL-25 is temporally up-regulated in developing normal mammary glands and induces caspase-mediated apoptosis of breast cancer cells without affecting nonmalignant MECs either in culture or in mice. The reason behind the resistance of nonmalignant cells to IL-25 is the differential expression of the receptor, IL-25R, high in breast cancer cells but low or absent in nonmalignant MECs (Fig. 5, A and B). IL-25R overexpression contributes to tumorigenic potential, as shown by the result that siRNA-induced reduction in the amounts of IL-25R impaired breast cancer cells' anchorage-independent growth in soft agar (Fig. 5, C to E). Examination of breast cancer specimens showed distinct up-regulation of IL-25R in 19% of the samples, correlating strongly in those with poor prognosis (Fig. 5I).

The exact mechanism by which IL-25R expression confers a growth advantage to breast cancer cells remains to be determined. We postulate that although IL-25R–expressing cancer cells do not express the apoptotic ligand IL-25 (Fig. 2A and fig. S4A), they may express another ligand that contributes to their tumorigenic potential. Such a candidate ligand appears to be IL-17B, which binds IL-25R with a markedly lower affinity than that of IL-25 (11). We found that IL-17B was expressed in most breast cancer cell lines that expressed high amounts of IL-25R, whereas IL-17B was absent from nonmalignant MCF10A cells (fig. S4A). Consistently, IL-17B was up-regulated in 30% of breast cancer specimens examined (12 of 40), but undetectable in normal tissues (0 of 18) (fig. S4B). Small hairpin RNA (shRNA)–dependent reduction of IL-17B amounts in MDA-MB468 breast cancer cells impaired their growth and invasive potentials (fig. S4, C to G), whereas ectopic addition of IL-17B protein enhanced both potentials (fig. S4, H to J). These results in sum suggest that IL-17B may augment the tumorigenicity of breast cancer cells in an autocrine manner. This possibility is presently under investigation. Whether IL-17B competes directly with IL-25 for receptor binding is not known. However, it is known that both IL-25 and IL-17B bind the extracellular domains of IL-25R in vitro, but that the IL-25 ligand shows a markedly higher affinity for the IL-25R than does IL-17B (11). Accordingly, it is speculated that IL-25 binding to the receptor would outcompete IL-17B if both were present simultaneously in the same cells. Some of our data, in fact, suggest that when both ligands are present, IL-25 binding to IL-25R is dominant over IL-17B binding to IL-25R. Figure S4A shows that IL-17B is expressed in most cancer cell lines tested. Yet, ectopic addition of IL-25 still causes the cells to apoptose. Nevertheless, the question could arise that if IL-25 has such a

strong affinity for IL-25R and this binding induces apoptosis, why would tumors ever have a chance to form? We hypothesize that it is the localization and/or temporal availability of each of these ligands that accounts for the fact that IL-25R–expressing tumors grow rather than apoptose. That is, once a tumor is formed, if IL-17B were to be present in the tumor, it would act as a growth promoter. Because IL-25 is not generated by the tumor cells, IL-25–dependent apoptosis would be absent.

In lymphoid and renal cells, IL-25R activation by IL-25 induces a proinflammatory response mediated by TRAF6; in these two tissue contexts, TRAF6 associates with its cognate binding domain in IL-25R and activates nuclear factor κB (NF-κB), which in turn stimulates the transcription of genes that encode inflammatory cytokines (11, 22). In contrast, IL-25R activation by IL-25 in breast cancer cells causes the receptor to interact with DD adaptor proteins FADD and TRADD, rapidly activating caspases 8 and 3 sequentially for apoptotic signaling (Fig. 6, D to G). This action appears to be mediated by the DD-like region in the C terminus of IL-25R. Constitutive binding of TRAF6 to IL-25R confers a protective effect on breast cancer cells, inhibiting apoptosis when IL-25 is not present (Fig. 7C). Such tissue-specific responses to IL-25/IL-25R signaling may result from additional proteins that serve as switches between TRAF6/NF-κB signals and TRADD/FADD/caspase 8 signals. This type of molecular switching has been shown previously for the related receptor, TNF-R1, which shares about 30% DD homology with IL-25R (Fig. 6A). TNF-R1 activation by TNF-α induces both NF-κB activation and apoptosis. However, NF-κB activation can be blocked by the brain- and reproductive organ–expressed (BRE) protein, which binds the juxtamembrane cytoplasmic region of TNF-R1 and promotes apoptotic signaling (27). It is anticipated that proteins with similar pathway-switching functions will be discovered in the IL-25 pathway.

IL-25 thus holds promise as the basis for development of novel, effective breast cancer therapeutics with broad therapeutic windows. Our demonstration of the marked effect of IL-25 administration in inhibiting tumor growth with no apparent toxicity to the normal tissues in animals (Fig. 4, C and D) and the correlation of IL-25R expression with poor prognosis in breast cancer patients support this contention. Unlike conventional immunotherapy in which a cytokine, such as IL-2, is administered by intravenous infusion (28) to provoke global immunologic responses (29), a therapy that targets IL-25/IL-25R signaling would induce apoptosis specifically in cancer cells that express IL-25R. Expression of IL-25R in 19% of invasive ductal carcinomas places this receptor in a class of markers of interest for therapeutic targeting because of its prevalence, correlation with aggressiveness, and cell surface location. In these aspects, IL-25R could be compared to Her2/neu (30). Targeting Her2/neu has become an important strategy for treating HER2+ breast cancers by means of trastuzumab, a monoclonal antibody that binds and inhibits Her2/neu, resulting in tumor regression. The findings reported here suggest that targeting IL-25R in patients bearing tumors that overexpress this receptor should similarly result in strong clinical responses. We anticipate that our present study will lead to the development of IL-25R–based diagnostics, facilitating identification of the target population, and IL-25/IL-25R–based therapeutics, such as IL-25 peptidomimetics or IL-25R antagonistic antibodies, to efficiently and specifically induce target cell apoptosis in patients with advanced breast cancer.

MATERIALS AND METHODS

See the Supplementary Material for the detailed Materials and Methods.

Supplementary Material

Refer to Web version on PubMed Central for supplementary material.

Acknowledgments

We are grateful to C. Hines and R. Wei for providing reagents and J. Mott, A. Lo, E. Y. Lee, A. D. Borowsky, and D. Brownfield for helpful comments. We thank E. Lee and X. Tian for technical assistance and R. Baehner and L. Chan (UCSF Comprehensive Cancer Center) for pathological analyses of the second cohort. **Funding:** This work was supported by grants from the NIH (RO1CA94170 to W.-H.L. and GM-74830 to L.H.), the National Cancer Institute (R37CA064786, U54CA126552, R01CA057621, U54CA112970, U01CA143233, and U54CA143836 to M.J.B.), the U.S. Department of Energy (DE-AC02-05CH1123 to M.J.B.), the U.S. Department of Defense (W81XWH0810736 to M.J.B. and W81XWH-05-1-0322 to S.F.), and a physician scientist award from the National Health Research Institute in Taiwan (to Y.-M.J.).

REFERENCES AND NOTES

1. Furuta S, Wang JM, Wei S, Jeng YM, Jiang X, Gu B, Chen PL, Lee EY, Lee WH. Removal of BRCA1/CtIP/ZBRK1 repressor complex on ANG1 promoter leads to accelerated mammary tumor growth contributed by prominent vasculature. Cancer Cell. 2006; 10:13–24. [PubMed: 16843262]
2. Bourhis XL, Toillon RA, Boilly B, Hondermarck H. Autocrine and paracrine growth inhibitors of breast cancer cells. Breast Cancer Res. Treat. 2000; 60:251–258. [PubMed: 10930113]
3. Barsky SH, Karlin NJ. Myoepithelial cells: Autocrine and paracrine suppressors of breast cancer progression. J. Mammary Gland Biol. Neoplasia. 2005; 10:249–260. [PubMed: 16807804]
4. Gudjonsson T, Rønnov-Jessen L, Villadsen R, Rank F, Bissell MJ, Petersen OW. Normal and tumor-derived myoepithelial cells differ in their ability to interact with luminal breast epithelial cells for polarity and basement membrane deposition. J. Cell Sci. 2002; 115:39–50. [PubMed: 11801722]
5. Furuta S, Jiang X, Gu B, Cheng E, Chen PL, Lee WH. Depletion of BRCA1 impairs differentiation but enhances proliferation of mammary epithelial cells. Proc. Natl. Acad. Sci. U.S.A. 2005; 102:9176–9181. [PubMed: 15967981]
6. Weaver VM, Petersen OW, Wang F, Larabell CA, Briand P, Damsky C, Bissell MJ. Reversion of the malignant phenotype of human breast cells in three-dimensional culture and in vivo by integrin blocking antibodies. J. Cell Biol. 1997; 137:231–245. [PubMed: 9105051]
7. Muthuswamy SK, Li D, Lelievre S, Bissell MJ, Brugge JS. ErbB2, but not ErbB1, reinitiates proliferation and induces luminal repopulation in epithelial acini. Nat. Cell Biol. 2001; 3:785–792. [PubMed: 11533657]
8. Wang X, Chen CF, Baker PR, Chen PL, Kaiser P, Huang L. Mass spectrometric characterization of the affinity-purified human 26S proteasome complex. Biochemistry. 2007; 46:3553–3565. [PubMed: 17323924]
9. Cao Y, Lundwall A, Gadaleanu V, Lilja H, Bjartell A. Anti-thrombin is expressed in the benign prostatic epithelium and in prostate cancer and is capable of forming complexes with prostate-specific antigen and human glandular kallikrein 2. Am. J. Pathol. 2002; 161:2053–2063. [PubMed: 12466122]
10. Kalkunte S, Brard L, Granai CO, Swamy N. Inhibition of angiogenesis by vitamin D-binding protein: Characterization of anti-endothelial activity of DBP-maf. Angiogenesis. 2005; 8:349–360. [PubMed: 16400520]
11. Lee J, Ho WH, Maruoka M, Corpuz RT, Baldwin DT, Foster JS, Goddard AD, Yansura DG, Vandlen RL, Wood WI, Gurney AL. IL-17E, a novel proinflammatory ligand for the IL-17 receptor homolog IL-17Rh1. J. Biol. Chem. 2001; 276:1660–1664. [PubMed: 11058597]
12. Kumar S, Hanning CR, Brigham-Burke MR, Rieman DJ, Lehr R, Khandekar S, Kirkpatrick RB, Scott GF, Lee JC, Lynch FJ, Gao W, Gambotto A, Lotze MT. Interleukin-1F7B (IL-1H4/IL-1F7) is processed by caspase-1 and mature IL-1F7B binds to the IL-18 receptor but does not induce IFN-γ production. Cytokine. 2002; 18:61–71. [PubMed: 12096920]
13. Smallwood PM, Munoz-Sanjuan I, Tong P, Macke JP, Hendry SH, Gilbert DJ, Copeland NG, Jenkins NA, Nathans J. Fibroblast growth factor (FGF) homologous factors: New members of the

FGF family implicated in nervous system development. Proc. Natl. Acad. Sci. U.S.A. 1996; 93:9850–9857. [PubMed: 8790420]

14. Chen H, Shi S, Acosta L, Li W, Lu J, Bao S, Chen Z, Yang Z, Schneider MD, Chien KR, Conway SJ, Yoder MC, Haneline LS, Franco D, Shou W. BMP10 is essential for maintaining cardiac growth during murine cardiogenesis. Development. 2004; 131:2219–2231. [PubMed: 15073151]
15. Furuta S. unpublished material.
16. Kolls JK, Lindén A. Interleukin-17 family members and inflammation. Immunity. 2004; 21:467–476. [PubMed: 15485625]
17. Neve RM, Chin K, Fridlyand J, Yeh J, Baehner FL, Fevr T, Clark L, Bayani N, Coppe JP, Tong F, Speed T, Spellman PT, DeVries S, Lapuk A, Wang NJ, Kuo WL, Stilwell JL, Pinkel D, Albertson DG, Waldman FM, McCormick F, Dickson RB, Johnson MD, Lippman M, Ethier S, Gazdar A, Gray JW. A collection of breast cancer cell lines for the study of functionally distinct cancer subtypes. Cancer Cell. 2006; 10:515–527. [PubMed: 17157791]
18. Allred DC, Harvey JM, Berardo M, Clark GM. Prognostic and predictive factors in breast cancer by immunohistochemical analysis. Mod. Pathol. 1998; 11:155–168. [PubMed: 9504686]
19. Létuvé S, Lajoie-Kadoch S, Audusseau S, Rothenberg ME, Fiset PO, Ludwig MS, Hamid Q. IL-17E upregulates the expression of proinflammatory cytokines in lung fibroblasts. J. Allergy Clin. Immunol. 2006; 117:590–596. [PubMed: 16522458]
20. Hofmann K, Tschopp J. The death domain motif found in Fas (Apo-1) and TNF receptor is present in proteins involved in apoptosis and axonal guidance. FEBS Lett. 1995; 371:321–323. [PubMed: 7556620]
21. Baker SJ, Reddy EP. Modulation of life and death by the TNF receptor superfamily. Oncogene. 1998; 17:3261–3270. [PubMed: 9916988]
22. Maezawa Y, Nakajima H, Suzuki K, Tamachi T, Ikeda K, Inoue J, Saito Y, Iwamoto I. Involvement of TNF receptor-associated factor 6 in IL-25 receptor signaling. J. Immunol. 2006; 176:1013–1018. [PubMed: 16393988]
23. Loeb LA. Mutator phenotype may be required for multistage carcinogenesis. Cancer Res. 1991; 51:3075–3079. [PubMed: 2039987]
24. Kim MR, Manoukian R, Yeh R, Silbiger SM, Danilenko DM, Scully S, Sun J, DeRose ML, Stolina M, Chang D, Van GY, Clarkin K, Nguyen HQ, Yu YB, Jing S, Senaldi G, Elliott G, Medlock ES. Transgenic overexpression of human IL-17E results in eosinophilia, B-lymphocyte hyperplasia, and altered antibody production. Blood. 2002; 100:2330–2340. [PubMed: 12239140]
25. Moseley TA, Haudenschild DR, Rose L, Reddi AH. Interleukin-17 family and IL-17 receptors. Cytokine Growth Factor Rev. 2003; 14:155–174. [PubMed: 12651226]
26. Fort MM, Cheung J, Yen D, Li J, Zurawski SM, Lo S, Menon S, Clifford T, Hunte B, Lesley R, Muchamuel T, Hurst SD, Zurawski G, Leach MW, Gorman DM, Rennick DM. IL-25 induces IL-4, IL-5, and IL-13 and Th2-associated pathologies in vivo. Immunity. 2001; 15:985–995. [PubMed: 11754819]
27. Gu C, Castellino A, Chan JY, Chao MV. BRE: A modulator of TNF-α action. FASEB J. 1998; 12:1101–1108. [PubMed: 9737713]
28. Atkins MB, Lotze MT, Dutcher JP, Fisher RI, Weiss G, Margolin K, Abrams J, Sznol M, Parkinson D, Hawkins M, Paradise C, Kunkel L, Rosenberg SA. High-dose recombinant interleukin 2 therapy for patients with metastatic melanoma: Analysis of 270 patients treated between 1985 and 1993. J. Clin. Oncol. 1999; 17:2105–2116. [PubMed: 10561265]
29. Jackaman C, Bundell CS, Kinnear BF, Smith AM, Filion P, van Hagen D, Robinson BW, Nelson DJ. IL-2 intratumoral immunotherapy enhances $CD8^+$ T cells that mediate destruction of tumor cells and tumor-associated vasculature: A novel mechanism for IL-2. J. Immunol. 2003; 171:5051–5063. [PubMed: 14607902]
30. Hudis CA. Trastuzumab—mechanism of action and use in clinical practice. N. Engl. J. Med. 2007; 357:39–51. [PubMed: 17611206]

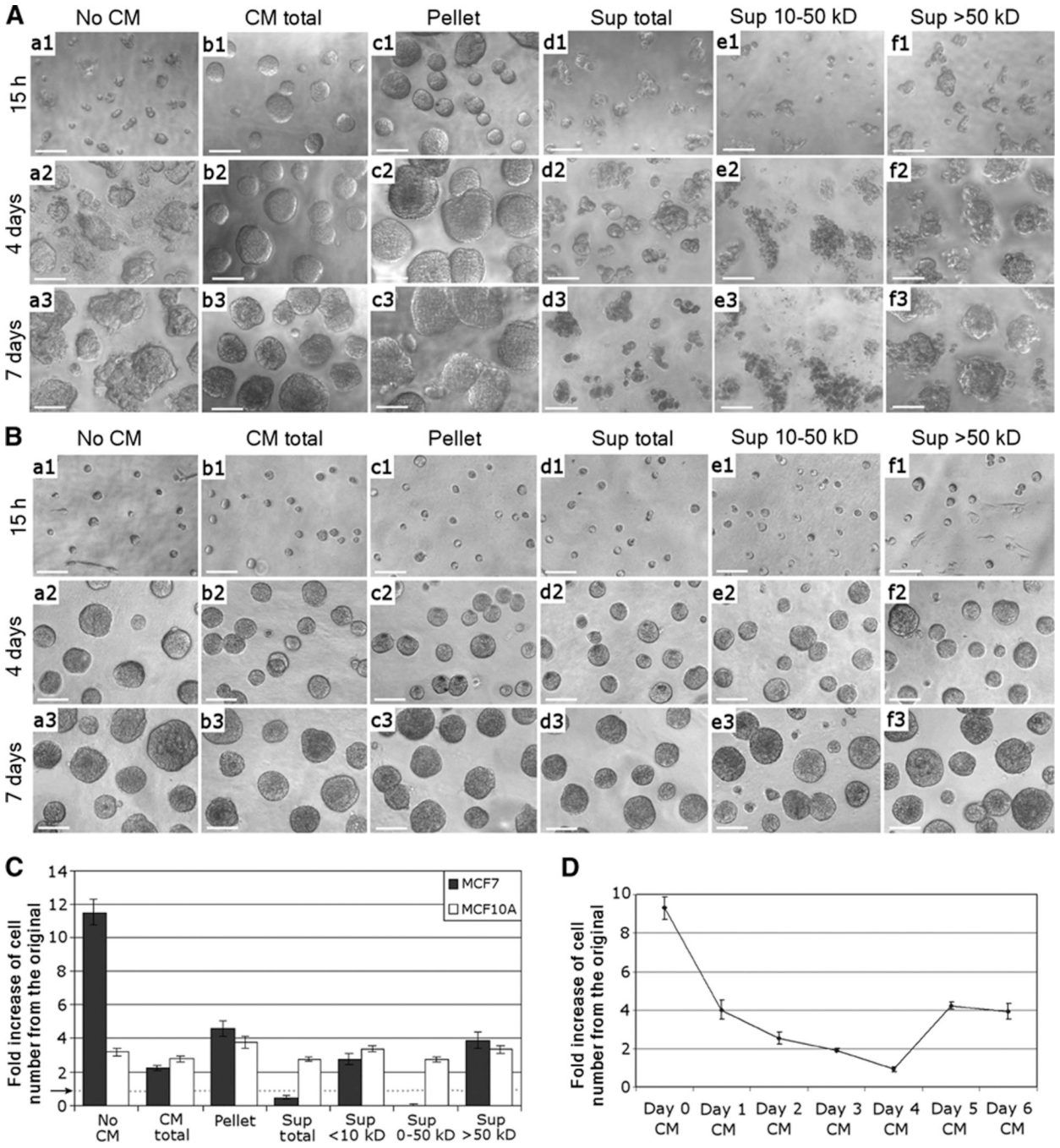

Fig. 1.

Fraction of CM (10- to 50-kD) from differentiating MECs exerts cytotoxicity on breast cancer cells in 3D cultures. (**A**) Morphologies of MCF7 cells cultured with (a) no CM, (b) total CM, (c) CM pelleted fraction, (d) CM total supernatant (Sup), (e) 10- to 50-kD fraction of CM, or (f) >50-kD fraction of CM for (1) 15 hours, (2) 4 days, or (3) 7 days on top of 3D lrECM. Cells were cultured on Matrigel layer with 2% Matrigel in medium. The control sample (a; no CM) was cultured with fresh MCF10A growth medium supplemented with 2% Matrigel. Scale bars, 50 μm. (**B**) Morphologies of MCF10A cells cultured under the same conditions and sampled at the same time periods as (A). (**C**) Numbers of viable MCF7 and MCF10A cells after 1 week in culture under the same conditions as (A). Error bars,

±SD. A dotted horizontal line, accentuated by an arrow, indicates the onefold line, the level at which the cells were seeded. (**D**) MCF10A CM was collected for 7 successive days in culture, and each 10- to 50-kD fraction was tested individually on MCF7 cells grown on 3D lrECM. The graph shows the number of viable cells after 7 days in culture in relation to the number of cells originally plated. $P < 0.05$.

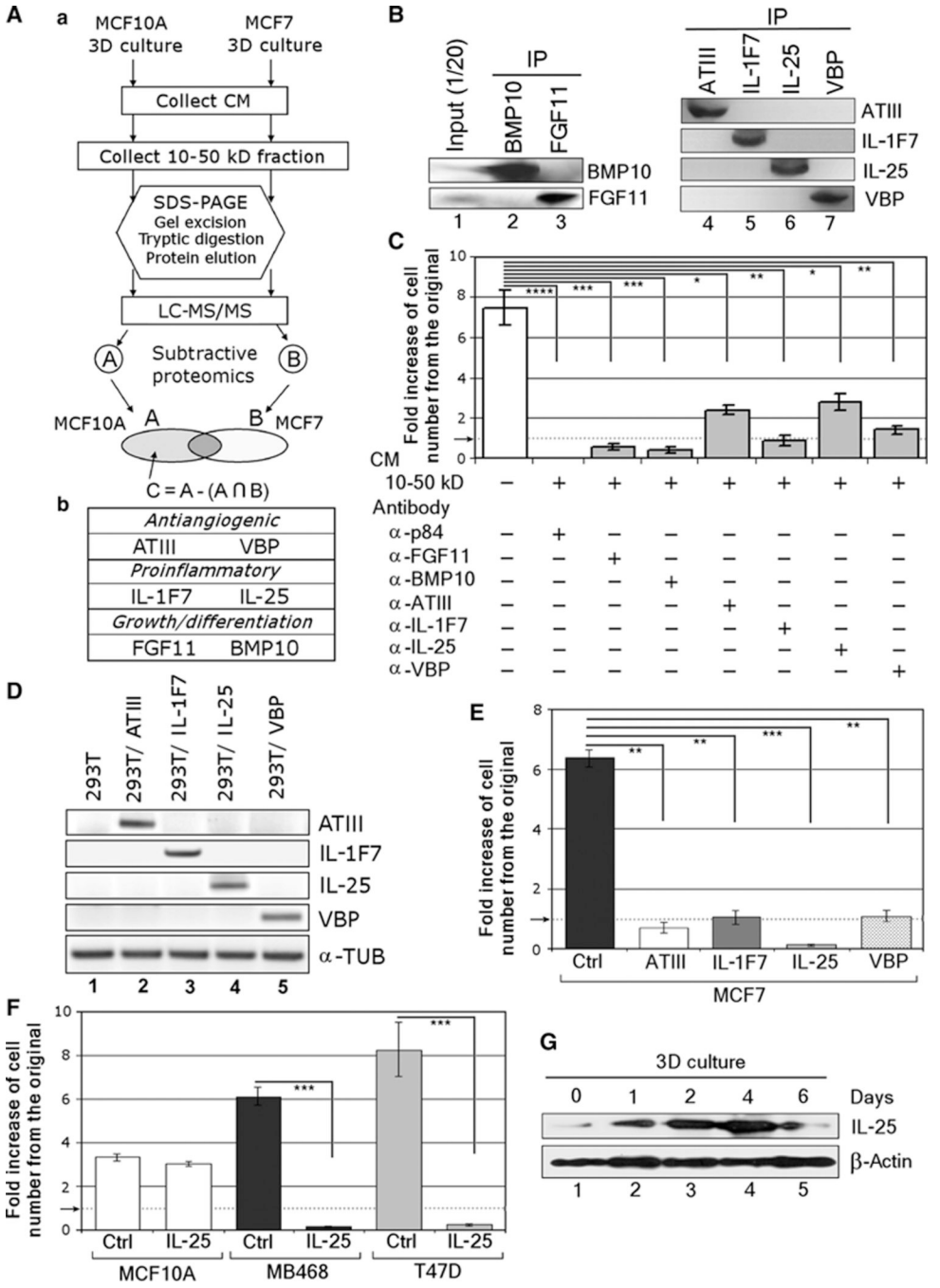

Fig. 2.

Subtractive proteomics identified IL-25 as a major tumor cell–killing component of the CM from differentiating MCF10A. (**A**) (a) Schematic for mass spectrometric analysis of CM. LC-MS/MS, liquid chromatography–tandem mass spectrometry; A∩B, A intersect B, components found in both A and B. (b) Six factors identified in the 10- to 50-kD fraction of CM at day 4 in culture. (**B**) Western blot analysis of immunoprecipitated (IP) factors to confirm the identity of BMP10, FGF11, ATIII, IL-1F7, IL-25, and VBP in the 10- to 50-kD fraction of day 4 CM. (**C**) Reduction in cytotoxicity of CM after immunodepletion. MCF7 cells were cultured in 3D lrECM with the 10- to 50-kD fraction of CM after immunodepletion of each of the six factors using p84 protein as a control (no reduction in

cytotoxicity). The numbers of viable cells in relation to the number of cells originally plated were counted after 1 week in culture. A dotted horizontal line, accentuated by an arrow, indicates the starting level at which the cells were seeded. Error bars, ±SD. $n = 4$. *$P < 0.05$; **$P < 0.01$; ***$P < 0.001$; ****$P < 0.0001$. (**D**) The four factors—ATIII, IL-1F7, IL-25, and VBP—showing the highest reduction in cytotoxicity after immunodepletion were stably overexpressed in 293T cells. The figure shows semiquantitative RT-PCR using α-tubulin (α-TUB) as an internal control. (**E**) IL-25 has the highest cytotoxicity: The CM produced by the 293T cells as in (D) was tested on MCF7 cells in 3D lrECM using CM from parental 293T cells as a control (Ctrl), and the numbers of viable cells were measured after 1 week in culture. The data are presented as fold increase in the cell number in relation to that originally plated. A dotted horizontal line, accentuated by an arrow, indicates the starting seeding density and marks the boundary between cytostatic and cytotoxic outcomes in our assay. Error bars, ±SD. $n = 4$. **$P < 0.01$; ***$P < 0.001$. (**F**) IL-25 exhibits cytotoxicity also on other breast cancer cell lines: A nonmalignant cell line (MCF10A) and two breast cancer cell lines (MDA-MB468 and T47D) were treated with CM fromthe 293T cells that overexpressed IL-25 and analyzed for viable cell numbers as in (E). A dotted horizontal line, accentuated by an arrow, indicates the starting seeding density. Error bars, ±SD. $n = 4$. ***$P < 0.001$. (**G**) Western blot analysis on the expression of IL-25 by differentiating acini in 3D culture. β-Actin serves as an internal control.

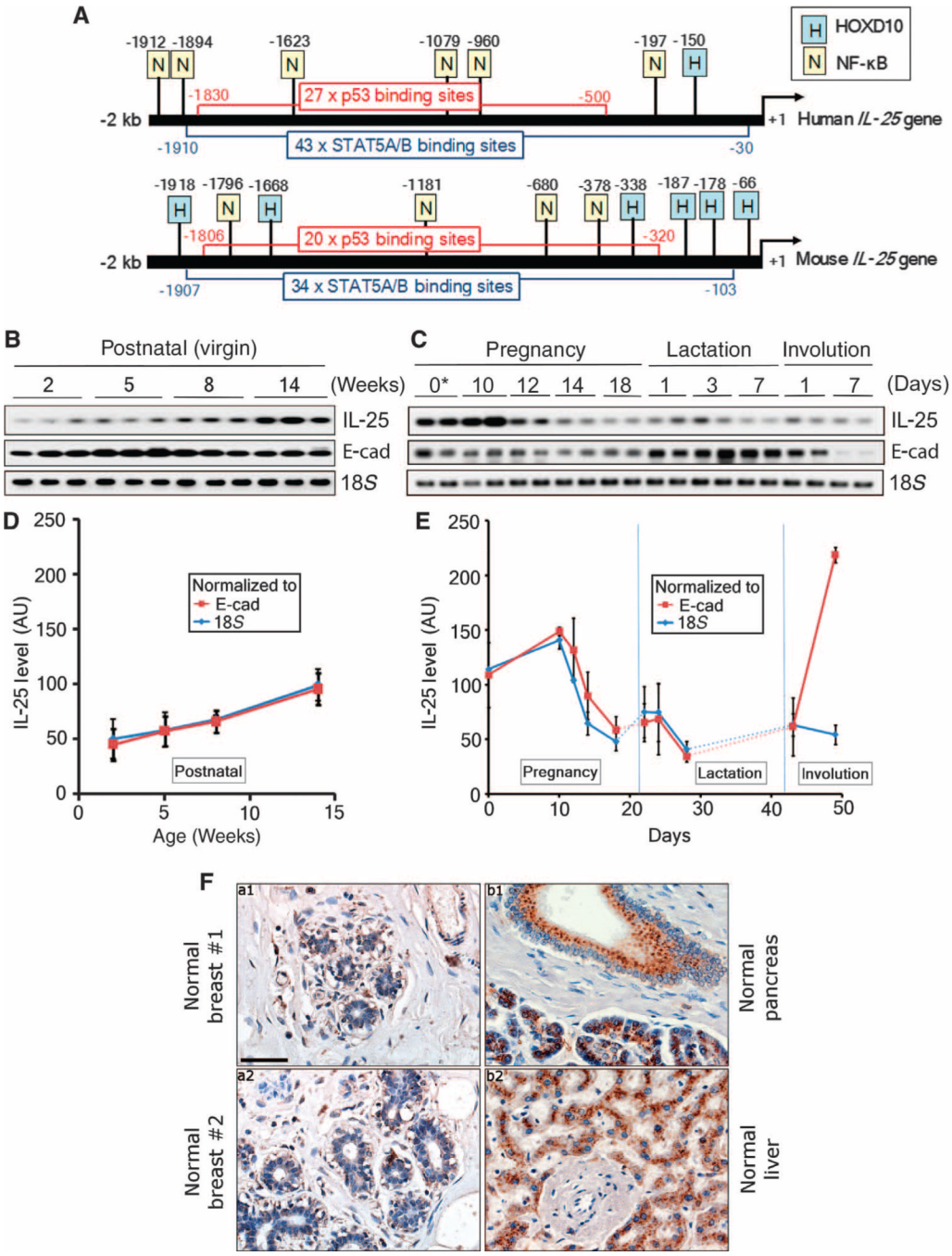

Fig. 3.

IL-25 is up-regulated during development of mammary gland but markedly reduced in mature human and mouse mammary glands. (**A**) Comparison of 2-kb regions upstream from the transcription start sites of human versus mouse *IL-25* genes. Transcription factor binding sites in these promoter regions were determined with PROMO 3.0.2 Web-based software. Note the presence of numerous binding sites for both p53 and STAT5A/B (signal transducer and activator of transcription 5A/B) in both human and mouse *IL-25* genes. (**B**) Expression levels of IL-25, E-cadherin (E-cad), and 18*S* in postnatally developing virgin mouse mammary glands at different time points (weeks). These levels were analyzed by semiquantitative RT-PCR. (**C**) Expression levels of IL-25, E-cad, and 18*S* in mouse

mammary glands at different stages of pregnancy and involution. These levels were analyzed by semiquantitative RT-PCR. Asterisk, 10 weeks old at day 0 of pregnancy. (**D**) Expression levels of IL-25 as in (B) normalized to E-cad or 18*S* by quantitative RT-PCR. (**E**) Expression levels of IL-25 as in (C) normalized to E-cad or 18*S* by quantitative RT-PCR. (**F**) Specimens of nontumorous human breast tissues ($n = 30$) (a1 and a2) were immunostained with a monoclonal antibody against IL-25. As positive controls, tissue sections from pancreas (b1) and liver (b2) were stained with the same antibody. Note that IL-25 staining in nontumorous breast tissues was almost undetectable. Scale bar, 50 μm.

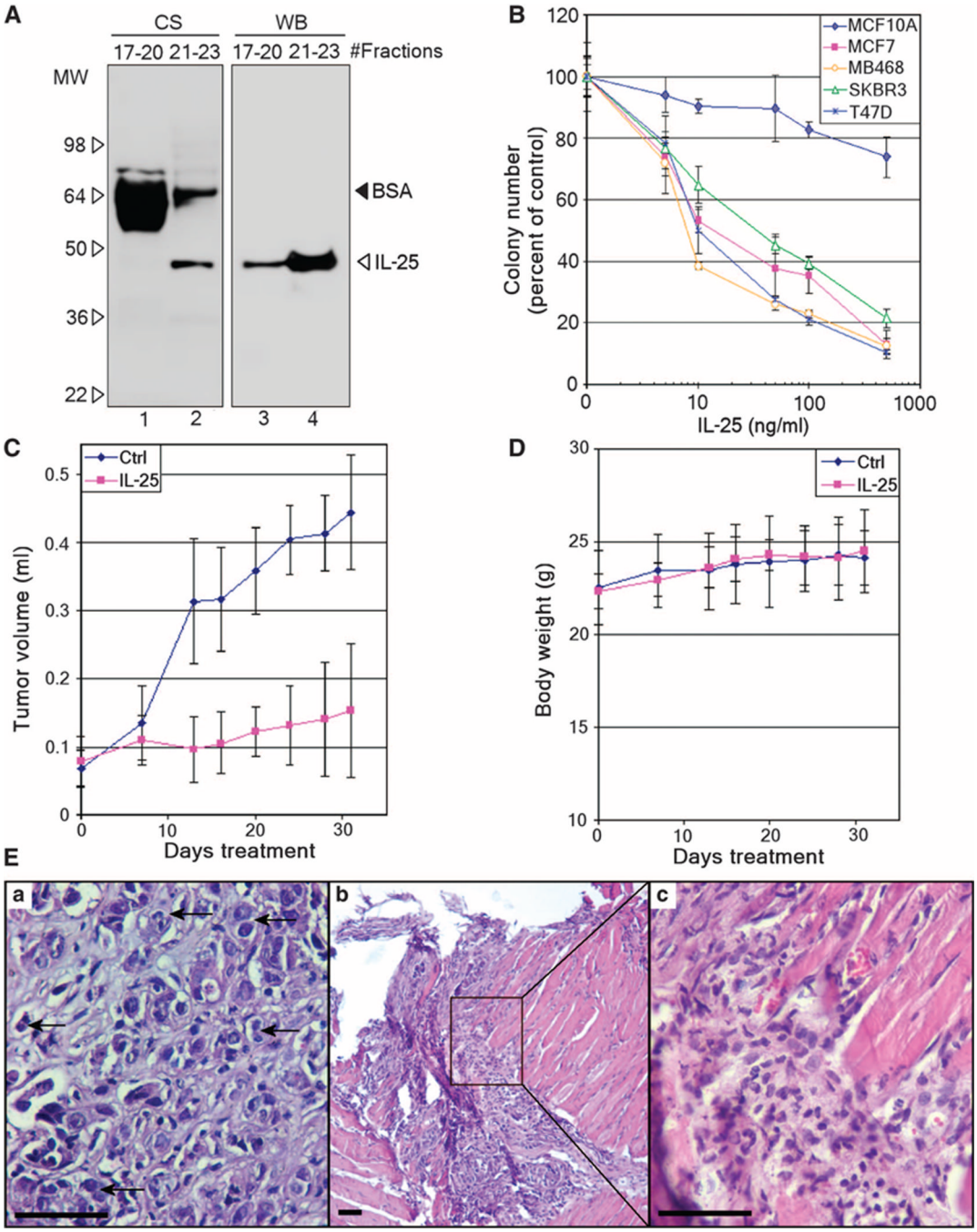

Fig. 4.

IL-25 exhibits cytotoxicity toward tumor cells both in colony assays and in vivo. (**A**) Secreted IL-25 protein was purified from the CM of overexpressing 293T cells via affinity purification of glycosylated proteins followed by gel filtration. Pooled gel-filtrated fractions containing glycosylated IL-25 (fractions 21 to 23) and other glycosylated proteins (fractions 17 to 20) were analyzed by Coomassie staining (CS, left) and Western blot (WB, right). Note the abundant bovine serum albumin (BSA) eluted in fractions 17 to 20 and its carryover in the IL-25 pool (fractions 21 to 23). MW, molecular weight. (**B**) Purified IL-25 protein described in (A) exhibits cytotoxicity on breast cancer cells. A nonmalignant cell line (MCF10A) and four breast cancer cell lines (MCF7, MDA-MB468, SKBR3, and T47D)

were treated with varying doses of IL-25, and the numbers of colonies formed were counted after 10 days in cultures. Error bars, ±SD. $n = 6$. (**C**) Purified IL-25 inhibits the growth of xenografted cancer cells. MDA-MB468 cells xenografted in the mammary fat pads of nude mice were treated with vehicle (control, $n = 7$) or IL-25 (300 ng, $n = 8$) for 31 days, and tumor sizes were measured twice weekly. $P = 0.0016$. Error bars, ±SD. (**D**) The body weights of mice described in (C) showed no differences throughout the experiment. Error bars, ±SD. $n = 7$ to 8. (**E**) Hematoxylin-eosin (H&E)–stained sections of (a) control and (b and c) IL-25–treated tumors as described in (C). The image (c) is a higher-magnification image of the boxed region in (b). Control sample shows actively growing tumor cells [representative entities are indicated with arrows in (a)], whereas in the IL-25–treated sample, the tumor was completely regressed and replaced with lymphocytic infiltrates [representative entities are shown in (c)]. Magnifications: ×400 (a and c); ×100 (b). Scale bars, 50 μm.

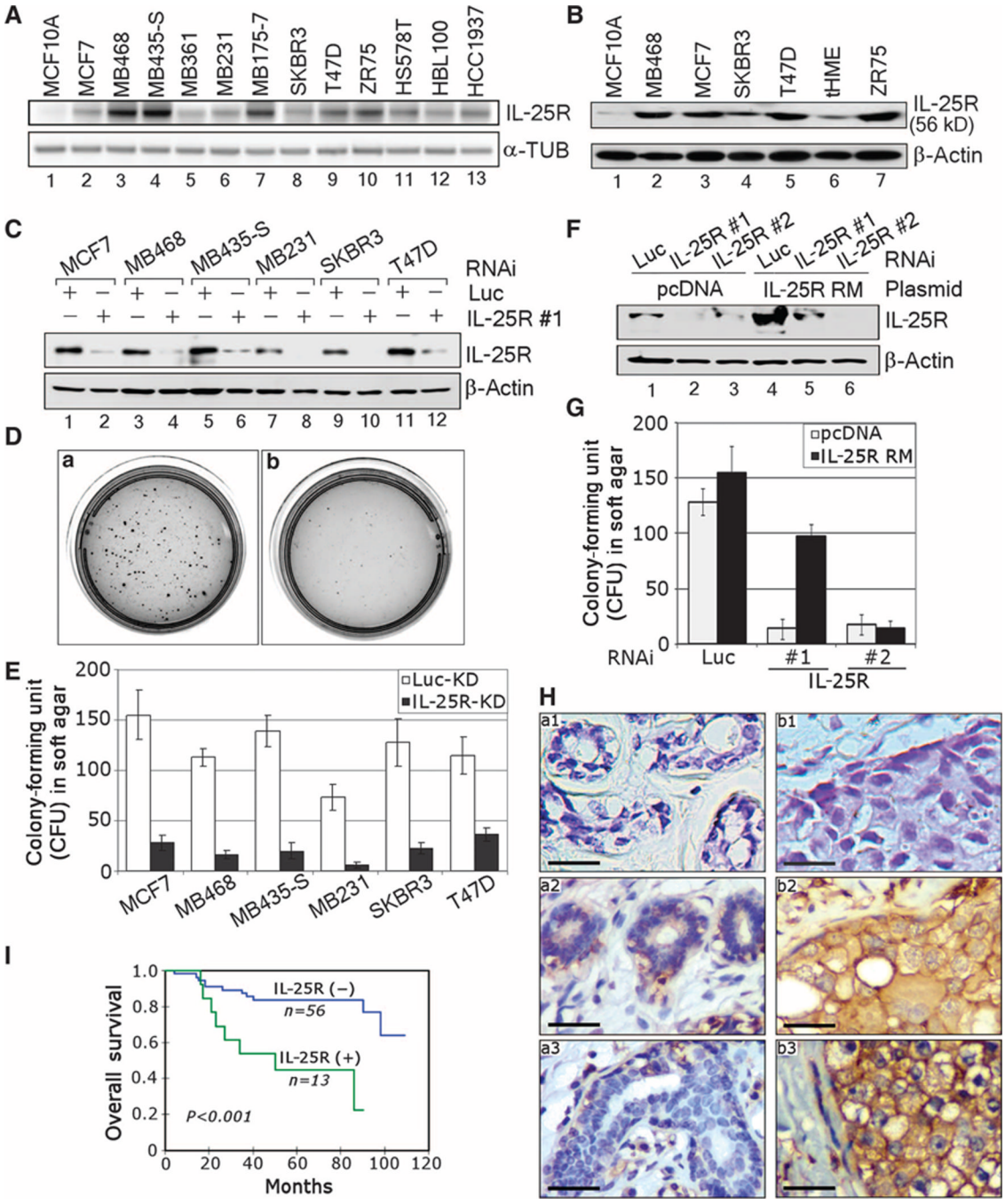

Fig. 5.

IL-25R is highly expressed in breast tumor cells, but not in nonmalignant MECs; the expression is involved in anchorage-independent growth ability of cells and inversely correlates with patients' prognosis. (**A**) RT-PCR analysis shows that breast cancer cell lines express higher amounts of IL-25R than nonmalignant breast cells. α-Tubulin (α-TUB) served as an internal control. (**B**) Western blot analysis confirms that IL-25R protein concentrations are higher in breast cancer cell lines than in nonmalignant breast cell lines. β-Actin served as an internal control. (**C**) Depletion of IL-25R in various breast cell lines with a specific siRNA. The Western blot confirms a decrease in IL-25R amounts in a panel of breast cancer cell lines (MCF7, MDA-MB468, MB435-S, MB231, SKBR3, and T47D) after

treatment with IL-25R siRNA. β-Actin served as an internal control. Luciferase (Luc) siRNA was used as a nonspecific control. (**D**) Down-modulation of IL-25R impairs the ability of SKBR3 cancer cells to grow on soft agar. Representative images of SKBR3 breast cancer cells grown for 2 weeks on soft agar after treatment with Luc siRNA (a) or IL-25R siRNA (b) as in (C). $n = 6$. (**E**) The number of colonies formed on soft agar decreases in breast cancer cells after treatment with IL-25R siRNA as in (D). Error bars, ±SD. KD, knockdown. (**F**) Expression of siRNA-resistant IL-25R restores IL-25R expression after siRNA treatment. Western blot analysis of IL-25R amounts in MDA-MB468 breast cancer cells expressing an IL-25R mutant (IL-25R RM) that is resistant to #1, but not #2, IL-25R siRNA after the cognate siRNA treatment. pcDNA plasmid was used as a vehicle control; Luc siRNA was used as a nonspecific siRNA control. (**G**) IL-25R RM expression rescues the soft agar growth ability of MDA-MB468 cells treated with IL-25R siRNA. Cells were transfected with vehicle or an IL-25R RM–expressing plasmid, treated with different siRNA constructs as in (F), and then analyzed for the numbers of colonies formed on soft agar. Error bars, ±SD. $n = 6$. (**H**) Specimens of nontumorous human breast tissue (a) versus human breast cancer (b) immunostained for IL-25R. Normal sample in upper left (a1) and tumor sample in upper right (b1) were both stained with an isotype-matched control IgG1 antibody, whereas the normal samples (a2) and (a3) and the tumor samples (b2) and (b3) were all stained with IL-25R antibody (GeneTex). Membranous staining of IL-25R was seen in tumor cells and surrounding inflammatory cells, but not in nonmalignant MECs. The images were captured at ×400 magnification. Scale bars, 25 mm. $n = 69$. (**I**) Survival analysis of patients with IL-25R(+) ($n = 13$) and IL-25R(−) ($n = 56$) tumors with XLSTAT-Life version 2007.4 software. Statistical significance was assessed with the log-rank test.

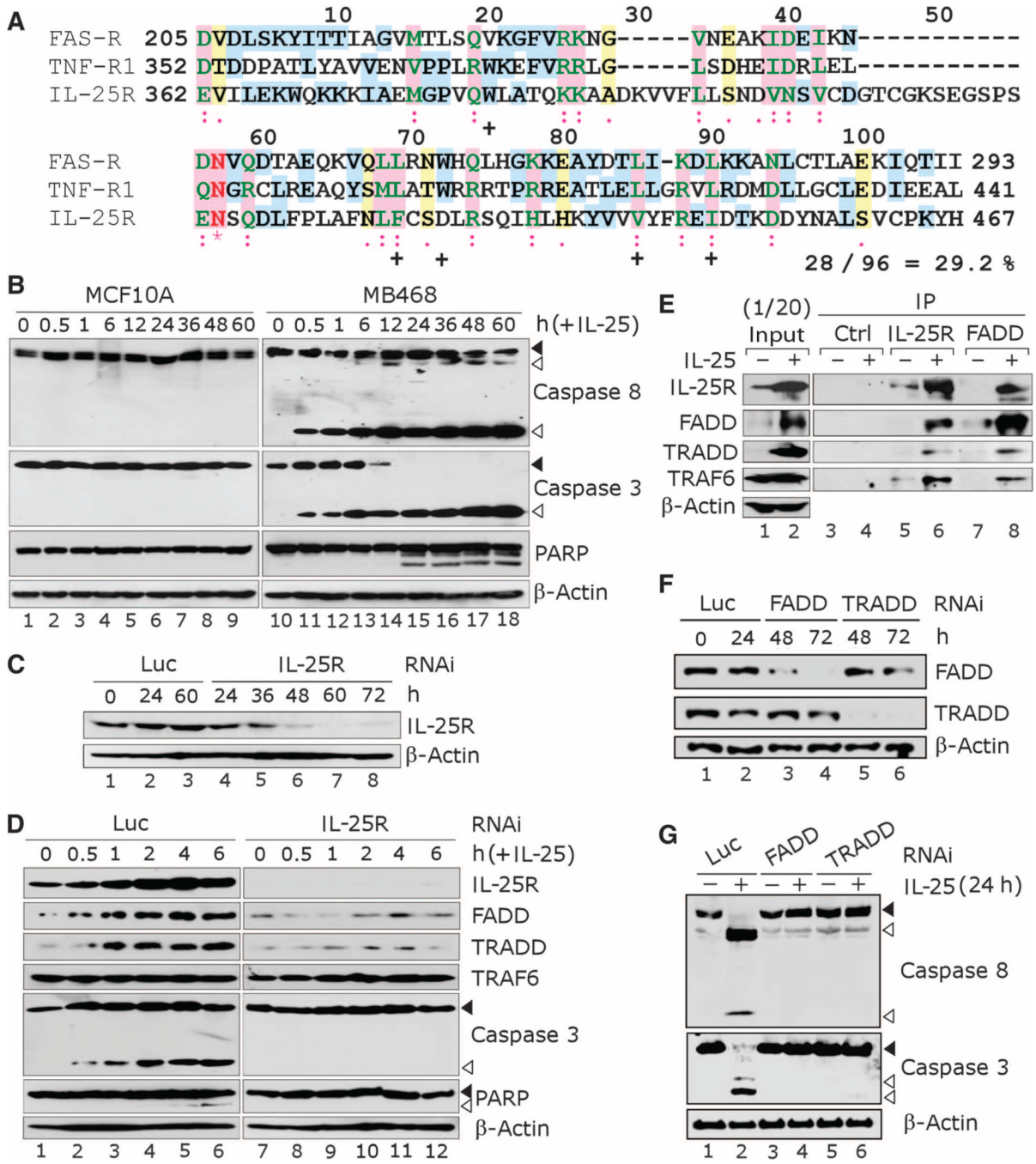

Fig. 6.

IL-25 induces apoptosis in breast cancer cells through receptor-mediated caspase activation. (**A**) IL-25R contains a death domain (DD)–like segment. Alignment of the C-terminal region of IL-25R (amino acids 362 to 467) with DDs of the FAS receptor (FAS-R, amino acids 205 to 293) and the TNF receptor 1 (TNF-R1, amino acids 352 to 441) with the ClustalW program shows similarity between the proteins. The amino acid residues within the aligned region are renumbered as indicated (1 to 106). (*) indicates identical residues; (:) indicates highly similar residues; (.) indicates similar residues; and (+) indicates residues that are highly conserved among DD-containing proteins (20). % Similarity = the sum of identical and similar residues/total residues. (**B**) IL-25 treatment induces apoptotic signaling in breast

cancer cells. Western blot analysis was used to detect the cleavage of caspases 8 and 3 and PARP in breast cancer cells (MDA-MB468) versus nonmalignant MECs (MCF10A) after treatment with IL-25 (500 ng/ml, ~25 nM) for varying periods of time. The cleavage products indicative of apoptosis are seen in MDA-MB468 cells, but not in MCF10A cells. β-Actin served as an internal control. Black arrowheads, uncleaved protein; white arrowheads, cleaved protein. (**C**) Western blot analysis confirms depletion of IL-25R in MDA-MB468 cells after IL-25R siRNA treatment. Luc siRNA was used as a nonspecific control; β-actin served as an internal control. (**D**) Depletion of IL-25R inhibits activation of proteins involved in apoptotic signaling. Western blot analysis was performed to detect the expression of effector proteins downstream of IL-25 signaling in MDA-MB468 cells treated with IL-25R siRNA versus Luc siRNA as in (C). β-Actin served as an internal control. Black arrowheads, uncleaved protein; white arrowheads, cleaved protein. (**E**) IL-25R associates with DD adaptor proteins upon IL-25 treatment. Coimmunoprecipitation analysis for the interaction of IL-25R with FADD, TRADD, and TRAF6; 1/20 of the input protein is shown. β-Actin served as an internal control. (**F**) Western blot analysis confirming the depletion of FADD or TRADD in MDA-MB468 cells after treatment with the cognate siRNAs. Luc siRNA was used as a nonspecific control; β-actin served as an internal control. (**G**) Depletion of FADD or TRADD impairs apoptotic activation in breast cancer cells upon IL-25 treatment. Western blot analysis showing the hindered cleavage of caspases 8 and 3 in MDA-MB468 cells treated with FADD or TRADD siRNA as in (F), and then exposed to IL-25 (500 ng/ml, ~25 nM) for 24 hours. β-Actin served as an internal control. Black arrowheads, uncleaved protein; white arrowheads, cleaved protein.

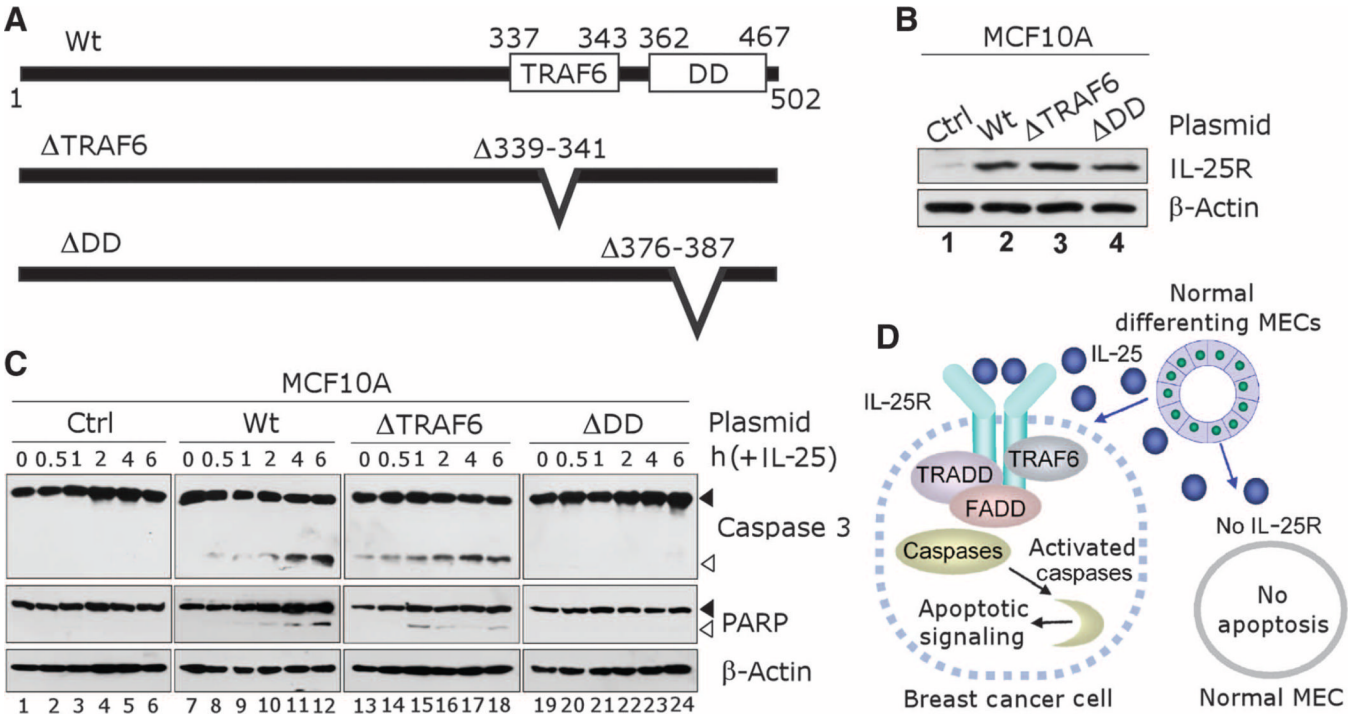

Fig. 7.

Death domain (DD)–like region of IL-25R renders cells sensitive to apoptotic signaling after treatment with IL-25. (**A**) Schematics for IL-25R protein expressed in mutation analyses. Wt, wild-type full-length IL-25R protein; ΔTRAF6, mutated IL-25R with a deletion in TRAF6 binding domain (amino acids Δ339–341); ΔDD, mutated IL-25R with a deletion in the DD-like region (amino acids Δ376–387). (**B**) Western blot shows that increased IL-25R amounts (Wt, ΔTRAF6, or ΔDD) after IL-25R were ectopically expressed in MCF10A cells compared to the endogenous IL-25R amounts in parental cells (Ctrl). β-Actin served as an internal control. (**C**) DD-like domain of IL-25R is essential for apoptotic signaling mediated by IL-25. Western blot analysis was used to detect cleavage of caspase 3 and PARP in MCF10A cells that expressed IL-25R as in (B) after treatment with IL-25 (500 ng/ml, ~25 nM) for varying time periods. β-Actin served as an internal control. Black arrowheads, uncleaved protein; white arrowheads, cleaved protein. (**D**) Schematic for the cytotoxic activity of IL-25 specific to breast cancer cells that express IL-25R. Nonmalignant MECs do not express IL-25R and are resistant to apoptosis induced by IL-25. Breast cancer cells that express IL-25R are susceptible to IL-25–induced apoptosis.